Research Article

Peng Wang*, Dietmar Auhl, Eckart Uhlmann, Georg Gerlitzky, and Manfred H. Wagner

Rheological and Mechanical Gradient Properties of Polyurethane Elastomers for 3D-Printing with Reactive Additives

https://doi.org/10.1515/arh-2019-0014
Received Sep 24, 2018; accepted Jun 11, 2019

Abstract: Polyurethane (PU) elastomers with their broad range of strength and elasticity are ideal materials for additive manufacturing of shapes with gradients of mechanical properties. By adjusting the mixing ratio of different polyurethane reactants during 3D-printing it is possible to change the mechanical properties. However, to guarantee intra- and inter-layer adhesion, it is essential to know the reaction kinetics of the polyurethane reaction, and to be able to influence the reaction speed in a wide range. In this study, the effect of adding three different catalysts and two inhibitors to the reaction of polyurethane elastomers were studied by comparing the time of crossover points between storage and loss modulus G' and G'' from time sweep tests of small amplitude oscillatory shear at 30°C. The time of crossover points is reduced with the increasing amount of catalysts, but only the reaction time with one inhibitor is significantly delayed. The reaction time of 90% NCO group conversion calculated from the FTIR-spectrum also demonstrates the kinetics of samples with different catalysts. In addition, the relation between the conversion as determined from FTIR spectroscopy and the mechanical properties of the materials was established. Based on these results, it is possible to select optimized catalysts and inhibitors for polyurethane 3D-printing of materials with gradients of mechanical properties.

Keywords: Polyurethane, oscillatory shear, crosslinking kinetics, infrared spectroscopy, 3D-printing

PACS: 61.41.+e, 82.35.-x, 83.10.Tv, 83.80.Va, 83.80.Jx

1 Introduction

Polyurethane (PU) elastomers with their broad range of strength and elasticity have found many applications in the past few decades, such as resins for automotive, medical, and aerospace industry. On the other hand, additive manufacturing is one of the fastest developing technologies and is challenging traditional manufacturing. In recent years, many different techniques of additive manufacturing have been developed for different polymers. For example, ABS, PLA and PC are commonly used materials for fused deposition modeling (FDM), while PA and PEEK are typical polymers for selective laser sintering (SLS) [1]. However, there are few researches on additive manufacturing of polyurethane based elastomers because only very few commercial devices can print polyurethane.

Elsner [2] has set up an inkjet printing prototype for additive manufacturing with piezoelectric nozzles, which can precisely adjust the ratio of two or more pre-polymer components by ejecting tiny amount of liquid. Müller *et al.* [3] studied the printability of polyisocyanate and polyols with this 3D-printing prototype. They demonstrated that by adjusting the mixing ratio of the polyurethane reactants it is possible to change the mechanical properties of each voxel, and established a technique of printing gradient materials. Uhlmann *et al.* [4, 5] investigated the printability of polyurethane further by optimizing the printing parameters, and managed to print small polyurethane cylinders by use of this prototype 3D-printing device (Figure 1).

Polyurethane materials are mainly obtained from a polyaddition reaction between di-isocyanates and polyols [6–8]. The basic reaction equation is shown as follows:

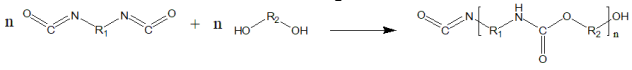

In this reaction, the hydroxyl groups of polyol lose a hydro-

***Corresponding Author: Peng Wang:** Department of Polymer Materials and Technologies, Technische Universität (TU) Berlin, Ernst-Reuter-Platz 1, D-10587 Berlin, Germany;
Email: peng.wang.1@tu-berlin.de
Dietmar Auhl, Manfred H. Wagner: Department of Polymer Materials and Technologies, Technische Universität (TU) Berlin, Ernst-Reuter-Platz 1, D-10587 Berlin, Germany
Eckart Uhlmann, Georg Gerlitzky: Department of Machine Tools and Factory Management, Technische Universität (TU) Berlin, Pascalstraße 8-9, 10587 Berlin, Germany

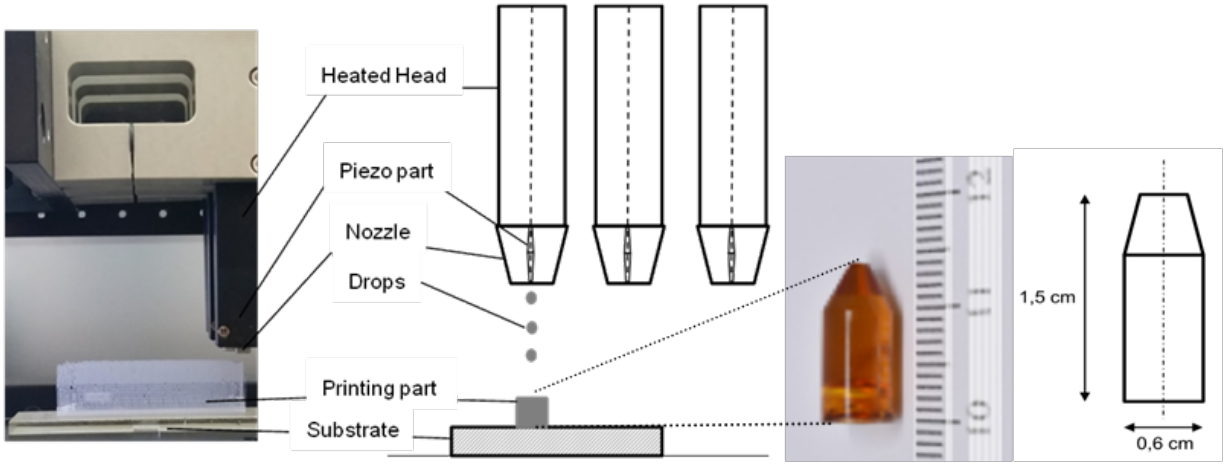

Figure 1: Prototype of 3D-printer and specimen of a 3D-printed test shape

gen atom and form an oxygen anion to connect with the carbon of isocyanate groups. The main effect of catalysts in this reaction is to help hydroxyl groups lose hydrogen ions. Common catalysts are amine-based 1,4-Di-Aza-Bi-Cyclo-(2,2,2)-Octane (DABCO), and tin-based Di-Butyl-Tin-Di-Laurate (DBTDL) [9]. Many studies [10–16] have already investigated the effects of these two types of catalysts onto the polyurethane formation reaction. The catalytic mechanism of DABCO is shown as follows for example:

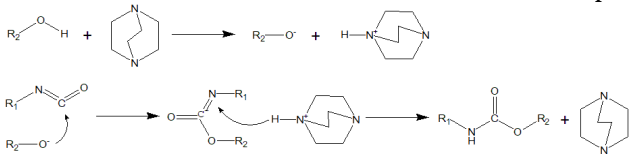

The function of an inhibitor is opposite to the action of catalysts, relying mostly on Lewis acids to hinder the proton transfer to the isocyanate groups. Commonly used inhibitors include Benzoyl-chloride and para-Toluene Sulfonic Acid (p-TSA) [17, 18], and these materials play an essential role in the pre-polymer preparation of polyurethane. However, it has also been noticed that the reaction can be accelerated by adding an excess of strong organic acids [19].

For the printing of polyurethanes, it is important to know the reaction time when the soft material is able to maintain a stable shape during the crosslinking reaction, because it determines when the next layer can be printed on the previous layer. Therefore, rheological characterization is an essential technique. By measuring the crossover point of storage modulus G′ and loss modulus G″ with constant amplitude and oscillatory frequency, this time can be determined and guaranteed precisely. Winter and Chambon *et al.* [20–25] have made great efforts in characterizing the gel point by rheological measurements for crosslinking polymers, including polyurethane. Moreover, Hu *et al.* [26] applied this method to bismaleimide/cyanate ester. They demonstrated that this method is practicable to compare the kinetics of a crosslinking reaction.

To characterize the overall polyaddition process of polyurethane, many studies have applied Fourier-transform infrared (FTIR) spectroscopy [27–30]. Particularly with the help of in-situ FTIR, one can observe the delay of the peak of the isocyanate group, and by comparison of isocyanate peak area and reference peak area, the conversion a of the NCO group can be calculated as shown in the following equation [31, 32]:

$$a = 1 - \frac{A_1(t)/A_2(t)}{A_1(0)/A_2(0)} \tag{1}$$

$A_1(0)$ and $A_1(t)$ are the peak areas of the isocyanate group at the beginning of the reaction and at time t, respectively; $A_2(0)$ and $A_2(t)$ are the reference peak areas at the beginning and at time t, respectively.

In this work, we investigate the effects of various reactive additives to the polyaddition reaction of polyurethane elastomers. For 3D-printing of reactive polymers like such polyurethanes, it is essential to be able to adjust the reaction rate, because the possible printing speed, especially in the vertical z-direction, relies on the reaction time until high viscous polymer is formed. By conducting time-dependent measurements with small-amplitude oscillatory shear (SAOS), it is possible to evaluate a processing time window from the dynamic mechanical response. Furthermore, the reaction process can be monitored also from conversion of chemical groups by FTIR spectroscopy. In addition, the mechanical properties of polyurethanes at different conversion stages are reported.

Table 1: Physical properties of Lupranol L1100, L3300, and Lupranat M20S according to the materials data sheet

	Hydroxyl value [mg KOH/g]	-N=C=O value [%]	Viscosity (25°C) [mPa·s]	Water Content [%]	Density (25°C) [g/cm^3]
Lupranol L1100	104	-	155	≤ 0.05	1.00
Lupranol L3300	400	-	373	≤ 0.10	1.05
Lupranat M20S	-	31.5	210	-	1.24

Table 2: Weight fraction of basic reactants with different catalysts and inhibitors

Reaction batch	M20S	L1100	L3300	DBTDL	Stannous octoate	DABCO	Benzoyl chloride	p-TSA
				[wt.%]				
PU-0	43.00	18.81	38.19	-	-	-	-	-
PU-L-0.01	42.99	18.81	38.19	0.01	-	-	-	-
PU-L-0.1	42.96	18.79	38.15	0.1	-	-	-	-
PU-L-0.2	42.92	18.77	38.11	0.2	-	-	-	-
PU-O-0.01	42.99	18.81	38.19	-	0.01	-	-	-
PU-O-0.1	42.96	18.79	38.15	-	0.1	-	-	-
PU-O-0.2	42.92	18.77	38.11	-	0.2	-	-	-
PU-A-0.01	42.99	18.81	38.19	-	-	0.01	-	-
PU-A-0.1	42.96	18.79	38.15	-	-	0.1	-	-
PU-A-0.2	42.92	18.77	38.11	-	-	0.2	-	-
PU-C-0.1	42.96	18.79	38.15	-	-	-	0.1	-
PU-C-2.5	41.95	18.35	37.26	-	-	-	2.44	-
PU-S-0.05	42.98	18.80	38.17	-	-	-	-	0.05
PU-S-0.1	42.96	18.79	38.15	-	-	-	-	0.1
PU-S-1	42.57	18.62	37.81	-	-	-	-	1

2 Experimental

2.1 Materials

Two polyols (Lupranol L1100 and Lupranol L3300, BASF Polyurethanes GmbH) and one polyisocyanate (Lupranat M20S, BASF Polyurethanes GmbH) were used as the main reactants and diluted by anhydrous toluene (Sigma-Aldrich). Lupranol L1100 is a difunctional polyol, which is used for production of foams and elastomers, and Lupranol L3300 is a trifunctional polyol based on glycerine, which is used for the production of rigid foams, but also for non-foamed polyurethane. Lupranat M20S is a solvent-free polyisocyanate, containing oligomers and isomers, which is mainly used for high-density rigid foams as well as for packing and casting materials. Lupranat M20W was used in a previous study [3], but is not commercially available any more, and therefore, Lupranat M20S is used as replacement with comparable properties. Table 1 presents the typical properties of the three main reactants.

Catalysts used as accelerating agents are Di-Butyl-Tin-Di-Laurate (DBTDL, Sigma-Aldrich), Tin(II)2-Ethyl-Hexanoate (also called Stannous Octoate, Sigma-Aldrich), and 1,4-Di-Aza-Bi-Cyclo-(2,2,2)-Octane (DABCO, Carl Roth GmbH), while inhibitors used are Benzoyl-Chloride (abcr GmbH) and para-Toluene-Sulfonic Acid (p-TSA, MP Biomedicals). The total amounts of each additive added to the reaction are shown as weight fractions in Table 2.

The molar ratio (MR) between the NCO group and the OH group as well as the polyol ratio (PR) has a significant effect on the reaction rate, and MR and PR are defined as

$$MR = \frac{\alpha_{NCO}}{\alpha_{OH}} \times 100 \tag{2}$$

where α_{NCO} and α_{OH} are number of moles of NCO and OH, respectively;

$$PR = \frac{m_{L1100}}{m_{L1100} + m_{L3300}} \tag{3}$$

where m_{L1100} and m_{L3300} are mass of L1100 and L3300, respectively.

In this work, the molar ratio was chosen to be 105, which is higher than 100, in order to release the rich of an

excess of isocyanate to react with water in air, forming allophonates [3]. From the results of tests conducted by time sweep tests in the rheometer for different polyol ratios, PR with 0.33 was chosen as the main polyol ratio in order to compare the effects of different reactive additives. All the reactants and tools were thoroughly dried in advance in a vacuum oven at a temperature of 50°C for 24 hours before preparation of samples. All compositions of reacting compounds investigated are shown in Table 2.

To prepare polyurethane reaction compounds, which can be printed with piezoelectric nozzles, Lupranol L1100, Lupranol L3300 and Lupranat M20S were firstly diluted by Toluene of 30 wt.%, 32 wt.% and 25 wt.%, respectively [3]. Then Lupranol L1100 and Lupranol L3300 were dropped in a neat beaker according to the mass fraction intended, and finally mixed. For rheological measurements, Lupranat M20S was poured into a disposable cup used under curing conditions. The polyol mixture was dropped into the polyisocyanate within 1 min. The reactants were stirred for 1 min and then transferred to the instrument. This is defined as the pure PU sample without catalysts or inhibitors.

For the sample preparation with additives, the catalysts were added after mixing of the three reactants, and then stirred for another 1 min before transfer to the instrument. When inhibitors were added, a certain amount of inhibitor needed to be dissolved in the polyol mixture in advance to form an acid liquid, and then it was added with the polyols to the reaction.

2.2 Rheological testing

The storage and loss modulus G′ and G″ as well as the crossover time were measured by using an Anton Paar MCR-301 rheometer with a CTD-450 oven chamber.

The time sweep tests were performed by plate and plate geometry with a diameter of 25 mm at a temperature of 30°C. To investigate the appropriate strain amplitude in linear viscoelastic region, amplitude sweep tests were first conducted for a strain range between 1% and 100% at an angular frequency of 0.5 rad/s. Time sweep tests were performed in controlled strain mode with 1% strain and at a frequency of 1 Hz. Rheological measurements were stopped much later than the crossover times, and repeated at least twice for every type of sample.

2.3 Fourier-Transform Infrared (FT-IT) Spectroscopy

The FTIR measurements were conducted on Thermo Nicolet 380 spectrometer with ATR mode to follow the conversion reaction. To maintain a reaction temperature of 30°C, a small oven was placed on the top of the ATR unit. After sufficient preheating for thermal equilibrium, the reaction liquid was dropped onto the diamond window measurements repeated with a certain time interval. This method mimics an in-situ measurement.

For the FTIR measurements, the samples were prepared with similar procedures as for the rheological testing. After the samples were stirred homogeneously, they were transferred with a pipette to the ATR crystal, and measured every 2 min for the first 10 min, then every 10 min for the first hour, every 20 min for the second hour, every 30 min for the third hour, every 60 min for the following time period until the absorbance of the NCO peak is lower than a relative intensity of 0.05.

2.4 Mechanical testing

The samples for the mechanical tests were prepared in a polytetrafluoroethylene (PTFE) mold, which was designed based on the international standard ISO 527-2 (Figure 2). After homogenously mixed, the reactants without additives were slowly casted into the mold to avoid the formation of bubbles. Then the mold with liquid reactants was shifted into a freezer with a temperature of about 5°C and kept there for 24 hours. This step slows down the crosslinking reaction and decreases the formation of bubbles. When taken out from the freezer, the samples have already become high viscous liquids and were subsequently stored in an oven at a temperature of 30°C.

When the samples had obtained a stable shape, they were demolded and kept at 30°C for further reaction. Before the tensile testing, three different points on the specimen were tested by FTIR to confirm its homogeneity in conversion (Figure 2), and the Shore A hardness was measured by a durometer. Afterwards, the samples were longitudinally stretched at a rate of 1 mm/min for the determination of the tensile modulus, and then by 100 mm/min for the remaining stress-strain diagram. The relationship between reaction conversion and corresponding mechanical properties was studied.

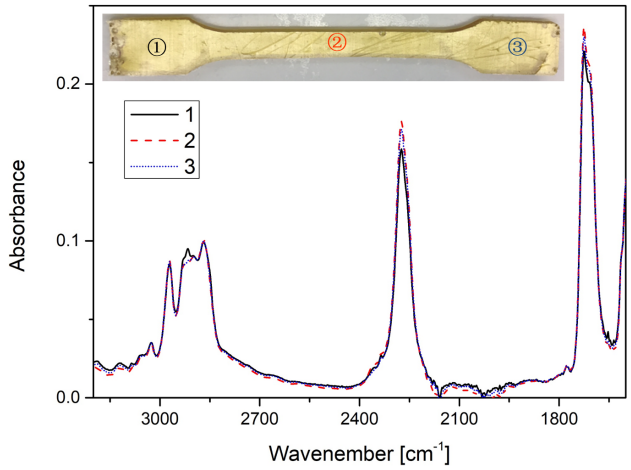

Figure 2: Tensile test specimen and corresponding FTIR spectrum at three different points

3 Results and discussion

3.1 Crosslinking behaviour from time sweep tests

Figure 3 shows for PU with different PRs the complex viscosities and dynamic moduli with changes in the G′ and G" crossover points. The curves show some characteristic regions and onset times, at which they grow with different rates. In Figure 3, the viscosities decreases with increasing amount of L1100 in the reaction, because L1100 has a low viscosity and can react with isocyanate, forming longer linear chains and networks with a low density of crosslinks. L1100 dilutes the reaction system and hinders the reaction between L3300 and isocyanate to form a 3-dimensional network structure. Therefore the sample with PR=0.66 needed the longest time to reach the crossover point. The compound with PR=0 has the highest growth rate of the three samples both for the viscosity and the moduli, because there are no diols in the reaction, which means that the resulting structure has more crosslinks than the other compounds. However, the resulting high viscosity slows down the reaction. Therefore, PR=0 needed more time to reach the crossover point than PR=0.33. By adding 33 wt.% of L1100, isocyanate forms more linear chains than PR=0 resulting in a lower viscosity, which in turn results in faster crosslinking with L3300. PR=0.33 is therefore the compound which reached the crossover point after the shortest reaction time. Since the compound with PR=0.33 has an earlier crossover point than other two compounds, it was chosen as the test compound in order to compare the effects of different catalysts and inhibitors.

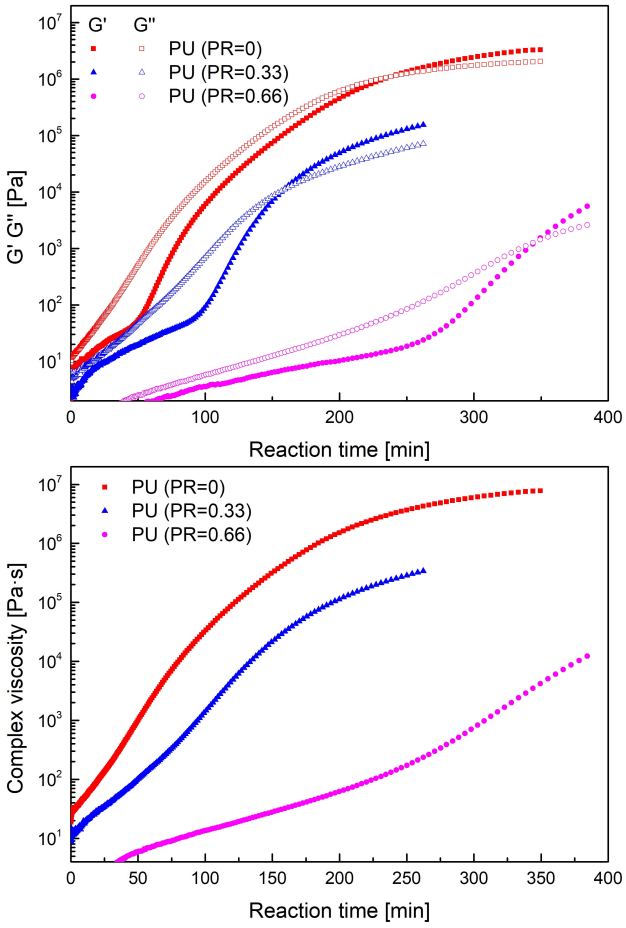

Figure 3: Time sweep results for storage and loss modulus G′ and G″ (left) as well as complex viscosity (right) for polyurethanes with PR of 0, 0.33, 0.66 without solvent

In the primary test for samples with different PRs, the pure reactants were used in bulk polymerization. As a result, the reaction heat was difficult to control, and the reaction heat accelerated the reaction between isocyanate and water in the air, forming a few bubbles. To decrease the viscosity for printing, the three reactants were diluted by toluene. In addition, toluene can absorb part of the heat produced by the reaction and isolates the water in the air from the reaction. Therefore, fewer bubbles were produced by the diluted reaction, and a higher G′/G" crossover point was obtained, but the time to reach the crossover point was extended to 612 min (black curve in Figure 4a-c) because of the decreased concentration of the reactants. Measured data of G′ and G″ at the start of the reaction were not reliable due to the extremely low viscosity, and they are not shown here.

From the diagrams, it can be seen that all the G′ curves have a similar shape and reach the level of 10^6 Pa, which means the crosslinking density of all samples are almost

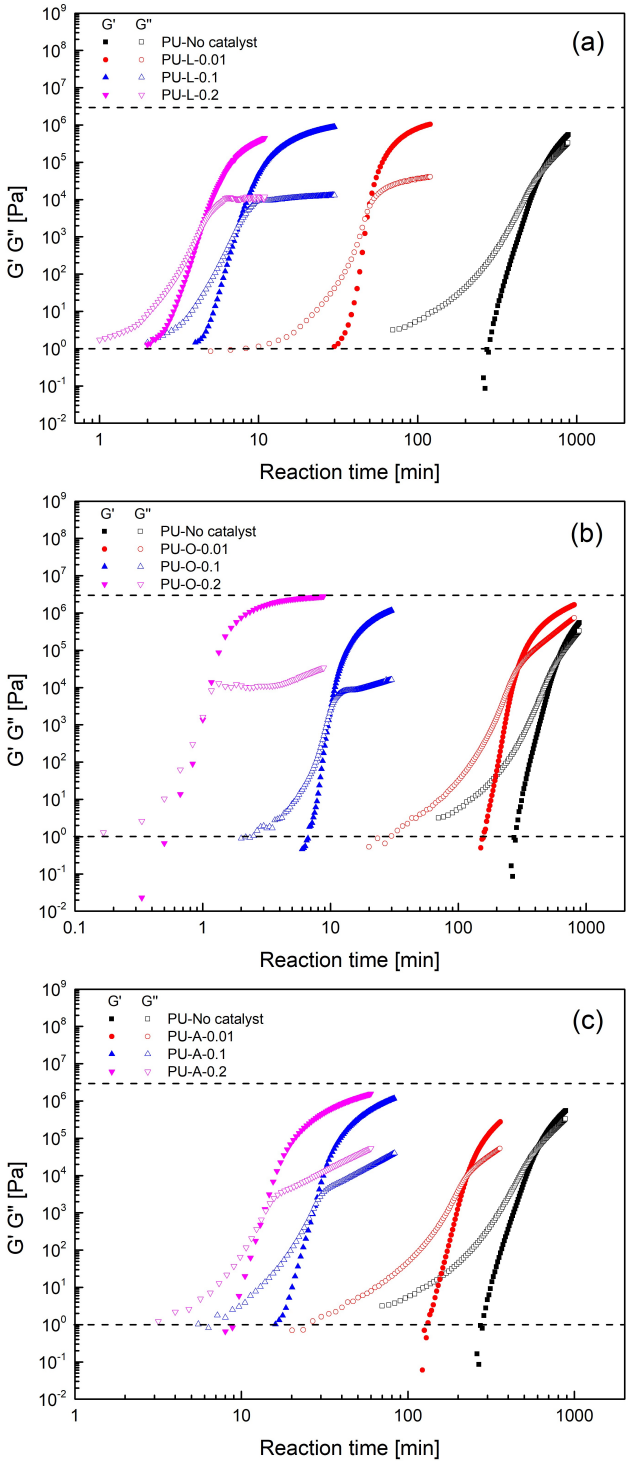

Figure 4: Time sweep tests for polyurethane compounds with no catalyst and with the different accelerating catalysts

identical, irrespective of the amount and type of catalyst used. However, the curves of G″ obviously differ after the crossover point. The samples with concentrations of 0.1 wt.% and 0.2 wt.% of catalyst show a pseudo-plateau (or

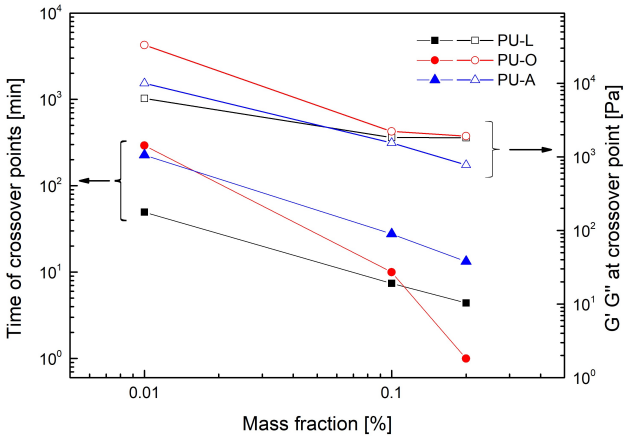

Figure 5: Time and value of G′ and G″ at crossover point as a function of mass fraction of each catalyst

slowly increasing) region with lower G″ values compared to the sample without catalyst. For example, G″ of the neat sample after the crossover point is approximately 10^5 Pa, but the loss modulus of the catalyzed samples reaches only 10^4 Pa. This may indicate that the three catalysts are efficient in producing a more perfect crosslinked network with fewer dangling ends.

Comparing the time to reach the crossover point in Figure 5, it is obvious that the time of samples with different amounts of catalyst L and A obey a power law, and L is more effective than A. This is because catalyst A is an amine-based catalyst, which not only improves the reaction between isocyanate and hydroxyl, but also the isocyanate-water reaction [19]. Stannous octoate (catalyst O) is a Tin-based complex compound. The results reveal that catalyst O has the lowest efficiency when a small amount (0.01 wt.%) is added, but is much more effective at higher concentrations. For the sample with 0.2 wt.% of O, the lowest crossover time is obtained.

Considering the value of G′ and G″ at the crossover point, the trend is first a decrease and then a plateau for catalyst L and O, while catalyst A still follows a power law. The decrease of the modulus values at the crossover point with increasing catalyst concentration is due to the fact that the catalysts create an efficient three-dimensional network.

To delay the curing time of this polyurethane, as typical inhibitors, Benzoyl chloride (inhibitor C) and para-Toluene-Sulfonic Acid (inhibitor S), were applied and their effects on the dynamic modulus are shown in Figure 6. Benzoyl chloride reacts with polyol of the system to form HCl. From the results, it is obvious that the time to reach the crossover point for the sample with 0.1 wt.% Benzoyl chloride is almost the same as for the sample without inhibitor,

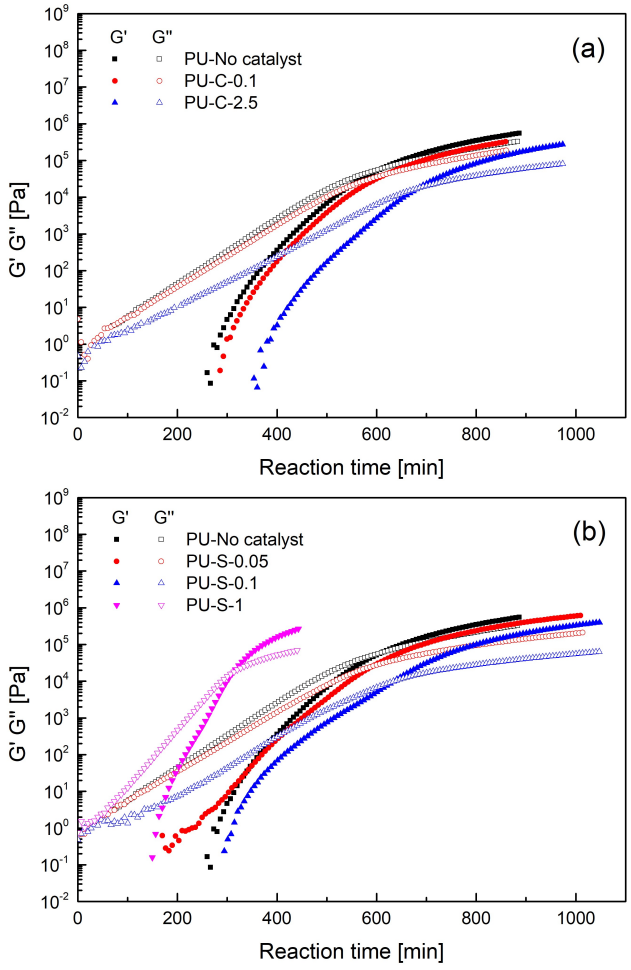

Figure 6: Time sweep tests for polyurethane reactions with different inhibitors Benzoyl-Chloride (a), and para-Toluene-Sulfonic Acid (b) compared to the sample without inhibitors

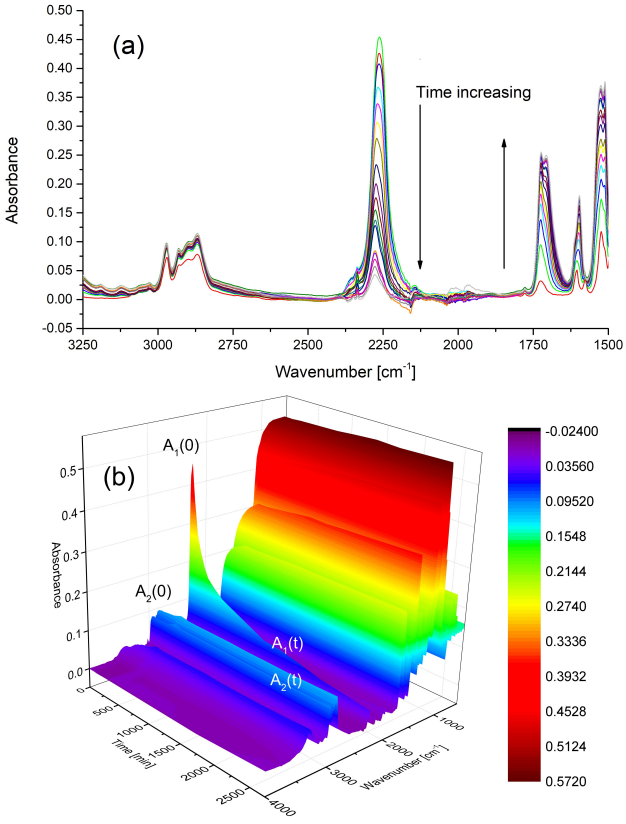

Figure 7: FTIR spectrum measured for the pure PU sample with PR=0.33 at different reaction times (a) and transformed into a 3-dimensional spectrum (b)

which means that such a small amount has only little effect on the reaction. If the amount of inhibitor is increased to 2.5 wt.%, it can delay the reaction more significantly. However, only poor reproducible results can be obtained for this amount because the reaction between Benzoyl chloride and polyol seems difficult to control.

Para-Toluene-Sulfonic Acid can be added directly to the reaction to vary the pH value. From Figure 6, it is seen that 0.05 wt.% has little effect as the time to the crossover point is nearly the same as without inhibitor. The most effective inhibitor amount is 0.1 wt.%, which results in a time of 634 min. However, when the amount is increased to 0.2 wt.%, the inhibitor may work as a catalyst, which reduces the time strongly to 312 min [19].

3.2 Degree of conversion from FTIR spectroscopy

Figure 7a shows the FTIR spectrum of the pure polyurethane PR=0.33 sample. The NCO group absorbance occurs between 2200-2350 cm^{-1} with a peak at 2280 cm^{-1} and as the reaction proceeds, the absorbance gradually drops. Figure 7b is the 3-dimensional spectrum transformed from Figure 7a. From this plot, it is obvious that the reaction rate of NCO is fast during the first 200 min, and then is reduced progressively because of the spatially hindering network structure and the high viscosity limiting the further reaction between functional groups. With the help of the reference peak at 2960 cm^{-1} for C-H stretching vibration in the CH_2 group of a polyether, the decrease of the peak area can be used to calculate the conversion of NCO group by use of equation 1 (Figure 8).

From Figure 8, it can be seen that the conversion of NCO group for polyurethanes with different reactive additives increases also sharply at the beginning of the reaction and then enters a plateau, which is similar to the pure PU as shown in Figure 7b. Compared to the starting point of

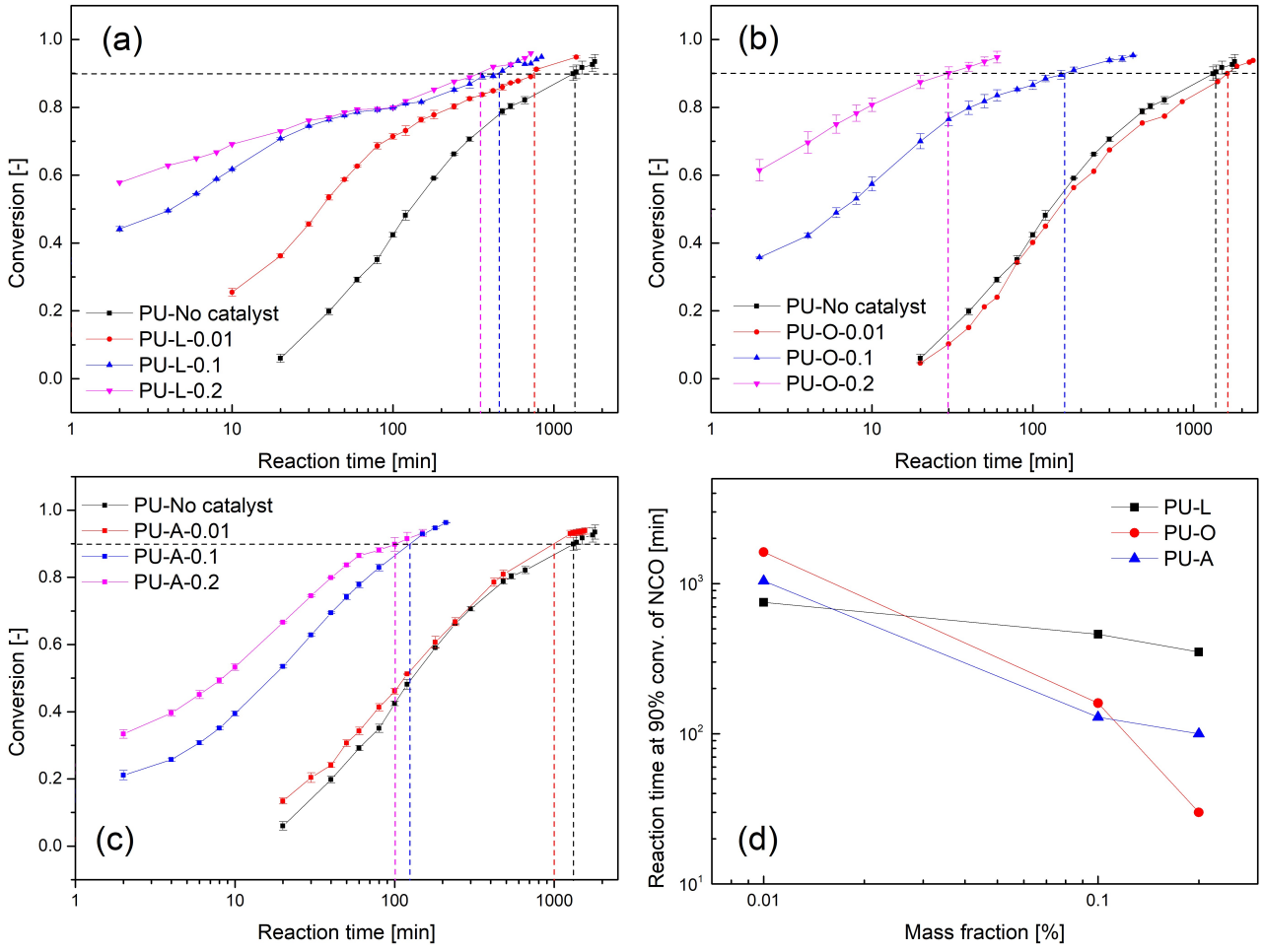

Figure 8: Conversion of NCO group for polyurethane with different reactive additives calculated from the FTIR spectrum (a-c). Reaction times to reach 90% conversion as a function of catalyst concentration (d)

the pure PU sample without catalyst, the starting points of PU with catalysts all have already a higher conversion, and with increasing amount of catalyst, the conversion is higher at comparable reaction times. This is because there is a certain loading time between adding the catalyst to the reaction compounds and the start of the measurements. This indicates that the catalysts have an obvious catalytic function during this loading time.

The catalysts L and O are both tin-based, but the efficiency is obviously different when compared at the same mass fractions. When 0.01 wt.% of L is added, the reaction time decreases to 815 min, which means that the reaction rate almost doubles. However, when the same amount of catalyst O is added, the reaction time is 1568 min, which is almost similar or even slightly longer than the time for the pure PU sample. This reveals that catalyst L is more effective than O at low mass fractions. Combined with the results from Figure 4b, it can be said that 0.01 wt.% of O is effective at the beginning of the reaction, but has no significant effects later during the reaction.

When the mass fraction is increased from 0.1 wt.% to 0.2 wt.%, the reaction time with addition of L is only reduced from 466 min to 341 min, which indicates that it is nearly saturated for this reaction. In contrast, when the mass fraction of catalyst O is increased to 0.1 wt.%, the reaction time decreases more than 10 times to 124 min, and when it is increased to 0.2 wt.%, the reaction time decreases almost another 10 times to 19 min. That means, for mass fractions above 0.1 wt.%, catalyst O is more effective than L. This may be explained in terms of the molecular structure, because O is sterically smaller than L, and therefore may diffuse much easier through the PU network to catalyze functional groups.

The addition of catalyst A with 0.01 wt.% results only in a small acceleration of the curing reaction, whereas with 0.1 wt.% and 0.2 wt.%, the reaction times are reduced to 136 min and 100 min, and possibly with 0.2 wt.% a satura-

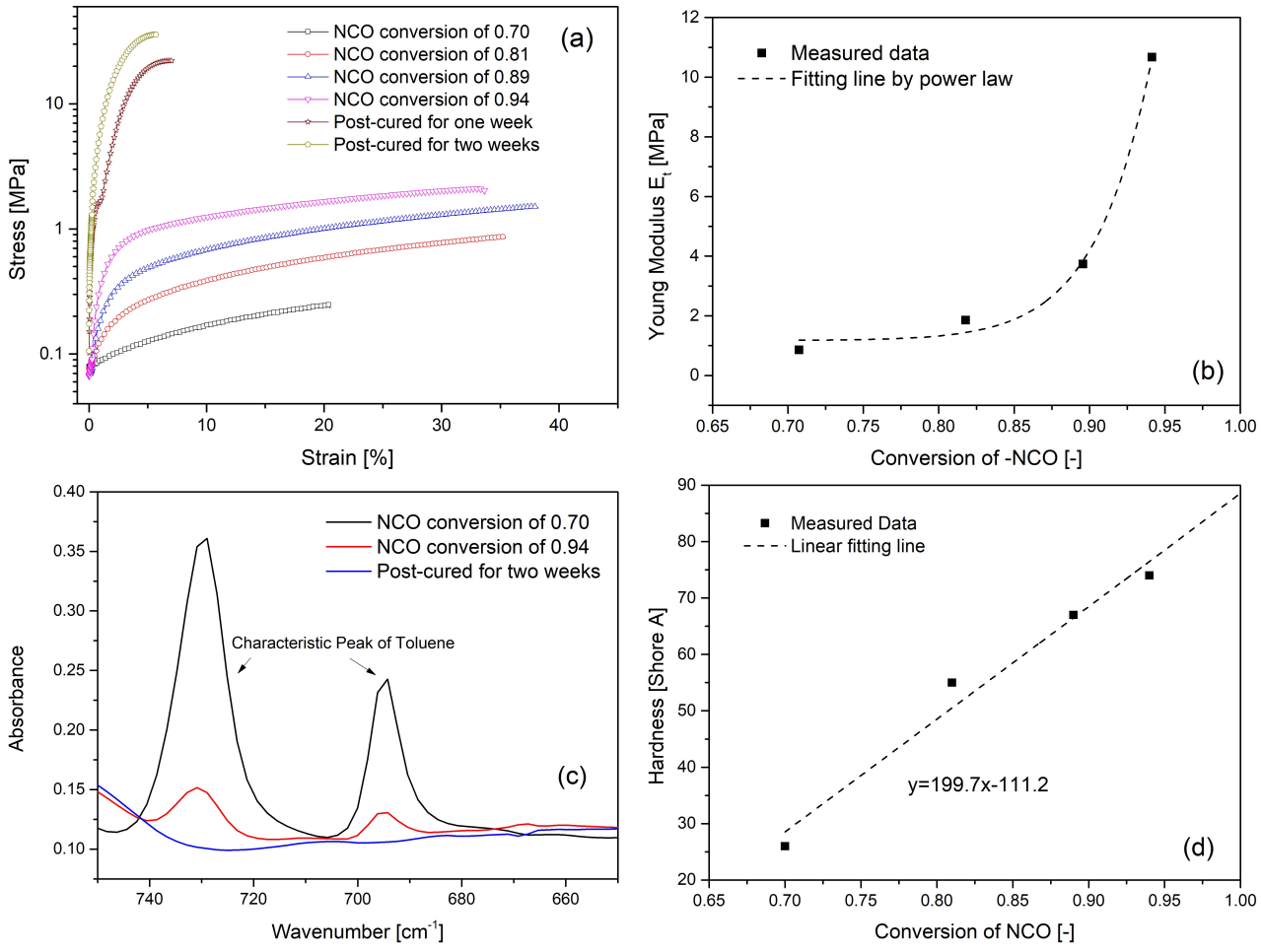

Figure 9: Tensile properties of PU with different degrees of NCO-conversion in stress-strain diagram (a), tensile modulus diagram (b), and characteristic peak of toluene in the FTIR spectrum (c), and Shore A hardness as a function of NCO-conversion (d)

tion concentration is already reached (Figure 8c). The summary of all reaction times of three accelerating catalysts is shown in Figure 8d.

3.3 Tensile properties and shore hardness

The changes of tensile properties of polyurethane elastomers are shown in Figure 9. It is found that the pure PU sample at crossover time of 612 min corresponds to a NCO group conversion of approximately 0.7. Thus, the first mechanical tests started at the conversion of 0.7. It can be seen that the elastomer with the lowest conversion 0.7 is extremely soft and weak. However, the stress-strain slope increases with higher degrees of conversion, while the strain at break has a trend to firstly increase and then to decrease. Two samples, which were post-cured for one week and two weeks, respectively, have significantly increased stresses at break (22 MPa and 36 MPa), but decreased strains at break (8% and 6%) compared to not fully reacted samples shown in Figure 9a.

Figure 9b shows the increase of tensile modulus for materials with increasing conversion. The increase is only small until a conversion of 0.85 is reached, but then increases significantly. The two post-cured samples have a much higher tensile modulus of 300 MPa and 396 MPa, respectively. This may also be largely due to the evaporation of toluene, because the characteristic peak of toluene in the FTIR spectrum (Figure 9c) decreases and finally disappears with continued post curing.

The Shore hardness of polyurethanes was measured at different degrees of conversion before tensile testing. However, hardness can be reliably measured only after passing the crossover point when the elastic response is dominating, *i.e.* when the conversion is larger than about 0.7. It is obvious that polyurethane turns harder subsequently because more crosslinks are created when the reaction proceeds. The growth trend can be fitted to a first approxima-

tion with a linear function (Figure 9d). If the function is extrapolated to full conversion of NCO, the result agrees relatively well with the Shore A hardness value of about 89 from previous work [3].

4 Conclusions

In this work, the effect of adding different reactive additives to the polyaddition reaction of polyurethane elastomers were studied by monitoring the crossover time of G′ and G″ in time sweep tests at 30°C. The crossover time is typically reduced with an increasing amount of accelerating catalyst, whereas the reaction time of some inhibitors is found to be delayed. The reaction progress was studied by FTIR spectroscopy for the NCO group conversion. In addition, the relation between the 90% NCO conversion as determined from the FTIR spectrum and the mechanical properties of the materials was established.

Concerning acceleration of the reaction rate, all three accelerating catalysts have good catalytic effects, which rise with increasing amount of catalysts. The two tin-based catalysts L and O are more efficient than the amine-based catalyst A. For mass fractions higher than 0.2 wt.% the catalyst O is the most effective additive.

The two inhibitors C and S have only a limited effect on delaying the reaction. Only S extends the crossover time to 634 min at a mass fraction of 0.1%. It seems that the acidic environment is able to inhibit the curing reaction of polyurethane to some extent.

Based on these results, it is possible to select optimized recipes with catalysts or inhibitors for 3D-printing with polyurethanes within large limits of reaction rate. With a certain ratio of reactants and additives, the printed layers can be adjusted to the printing time with improved or guaranteed intra-layer adhesion as well as to the time interval for inter-layer adhesion. After printing several layers, the load carrying capacity of the support layers also needs to be considered. Moreover, when the printing procedure is finished, the conversion diagram can be used to determine the time for removing the printed object.

With increasing conversion, characteristic mechanical properties such as hardness and tensile modulus of the polyurethane materials increased. These data are essential to set up process parameters for 3D-printing of polyurethane shapes, especially also with gradients in mechanical properties.

Thus, it is possible to optimize the 3D-printing process with respect to processing conditions as well as end-use properties. Yet, further inhibitors and recipes should be investigated in further detail in the future.

Acknowledgement: The authors would like to thank German Research Foundation (DFG) for financial support of this project by grants DFG Uh100/117-2, DFG Wa 668/332 and the Open Access Publication Fund of TU Berlin.

References

[1] Ligon S.C., Liska R., Stampfl J., Gurr M. and Mülhaupt R., Polymers for 3d printing and customized additive manufacturing, Chem Rev, 2017, 117, 10212-10290.
[2] Elsner P., 3D-Drucktechnologie–Grundlagen zur Herstellung polymerer Bauteile mit gradierten Werkstoffeigenschaften, Dissertation, Technische Universität Berlin, Berlin, Germany, 2009.
[3] Müller M., Huynh Q-U., Uhlmann E. and Wagner M.H., Study of inkjet printing as additive manufacturing process for gradient polyurethane material, Production Engineering, 2013, 8, 25-32.
[4] Uhlmann E., Wagner M.H. and Gerlitzky G., Additives Fertigungsverfahren zur Herstellung von Bauteilen mit Eigenschaftsgradienten, ZWF Zeitschrift für wirtschaftlichen Fabrikbetrieb, 2018, 113, 290-294.
[5] Uhlmann E., Wagner M.H. and Gerlitzky G., Additive Fertigung mittels 3D-Gradientendruck, Ingenieurspiegel, 2018, August.
[6] Feng X., Yusheng S. and Shuhuai H., Synthesis and performance of transparent casting polyurethane resin, Journal of Wuhan University of Technology-Mater. Sci. Ed., 2005, 20, 24-28.
[7] Chen X-D., Zhou N-Q. and Zhang H., Preparation and properties of cast polyurethane elastomers with molecularly uniform hard segments based on 2,4-toluene diisocyanate and 3,5-dimethylthioltoluenediamine, Journal of Biomedical Science and Engineering, 2009, 02, 245-253.
[8] Lligadas G., Ronda J.C., Galià M., Biermann U. and Metzger J.O., Synthesis and characterization of polyurethanes from epoxidized methyl oleate based polyether polyols as renewable resources, Journal of Polymer Science Part A: Polymer Chemistry, 2006, 44, 634-645.
[9] Krol P., Synthesis methods, chemical structures and phase structures of linear polyurethanes. Properties and applications of linear polyurethanes in polyurethane elastomers, copolymers and ionomers, Progress in Materials Science, 2007, 52, 915-1015.
[10] Fiori S., Mariani A., Ricco L. and Russo S., First synthesis of a polyurethane by frontal polymerization, Macromolecules, 2003, 36, 2674-2679.
[11] Pattanayak A. and Jana S.C., Synthesis of thermoplastic polyurethane nanocomposites of reactive nanoclay by bulk polymerization methods, Polymer, 2005, 46, 3275-3288.
[12] Niyogi S., Sarkar S. and Adhikari B., Catalytic activity of dbtdl in polyurethane formation, Indian Journal of Chemical Technology, 2002, 9, 330-333.
[13] Yang Y. and Urban M.W., Self-repairable polyurethane networks by atmospheric carbon dioxide and water, Angew Chem Int Ed Engl, 2014, 53, 12142-12147.
[14] Skrobot J., Zair L., Ostrowski M. and El Fray M., New injectable elastomeric biomaterials for hernia repair and their biocompati-

bility, Biomaterials, 2016, 75, 182-192.
[15] Mathew S., Baudis S., Neffe A.T., Behl M., Wischke C. and Lendlein A., Effect of diisocyanate linkers on the degradation characteristics of copolyester urethanes as potential drug carrier matrices, Eur J Pharm Biopharm, 2015, 95, 18-26.
[16] Yeganeh H. and Mehdizadeh M.R., Synthesis and properties of isocyanate curable millable polyurethane elastomers based on castor oil as a renewable resource polyol, European Polymer Journal, 2004, 40, 1233-1238.
[17] Krol B., Krol P., Pikus S., Chmielarz P. and Skrzypiec K., Synthesis and characterisation of coating polyurethane cationomers containing fluorine built-in hard urethane segments, Colloid Polym Sci, 2010, 288, 1255-1269.
[18] Braun D., Cherdron H., Rehahn M., Ritter H. and Voit B., Polymer synthesis: Theory and practice: Fundamentals, methods, experiments, Springer Science & Business Media, 2012.
[19] Sardon H., Pascual A., Mecerreyes D., Taton D., Cramail H. and Hedrick J.L., Synthesis of polyurethanes using organocatalysis: A perspective, Macromolecules, 2015, 48, 3153-3165.
[20] Chambon F. and Winter H.H., Stopping of crosslinking reaction in a pdms polymer at the gel point, Polymer Bulletin, 1985,13, 499-503.
[21] Winter H.H. and Chambon F., Analysis of linear viscoelasticity of a crosslinking polymer at the gel point, Journal of Rheology, 1986, 30, 367-382.
[22] Chambon F., Petrovic Z.S., MacKnight W.J. and Winter H.H., Rheology of model polyurethanes at the gel point, Macromolecules, 1986, 19, 2146-2149.
[23] Chambon F. and Winter H.H., Linear viscoelasticity at the gel point of a crosslinking pdms with imbalanced stoichiometry, Journal of Rheology, 1987, 31, 683-697.
[24] Winter H., Can the gel point of a cross-linking polymer be detected by the G′–G″ crossover?, Polymer Engineering & Science, 1987, 27, 1698-1702.
[25] Winter H.H., Morganelli P. and Chambon F., Stoichiometry effects on rheology of model polyurethanes at the gel point, Macromolecules, 1988, 21, 532-535.
[26] Hu X., Fan J. and Yue C.Y., Rheological study of crosslinking and gelation in bismaleimide/cyanate ester interpenetrating polymer network, Journal of Applied Polymer Science, 2001, 80, 2437-2445.
[27] Ketata N., Sanglar C., Waton H., Alamercery S., Delolme F., Paisse O., Raffin G. and Grenier-Loustalot M-F., Synthesis, mechanisms and kinetics of formation of bi-component polyurethanes, Polymers and Polymer Composites, 2004, 12, 645-665.
[28] Kröber P., Delaney J.T., Perelaer J. and Schubert U.S., Reactive inkjet printing of polyurethanes, Journal of Materials Chemistry, 2009, 19, 5234.
[29] Trovati G., Sanches E.A., Neto S.C., Mascarenhas Y.P. and Chierice G.O., Characterization of polyurethane resins by ftir, tga, and xrd, Journal of Applied Polymer Science, 2010, 115, 263-268.
[30] Gogoi R., Sarwar Alam M. and Khandal R.K., Effect of reaction time on the synthesis and properties of isocyanate terminated polyurethane prepolymer, Int. J. Eng. Res. Technol, 2014, 3, 1404-1411.
[31] Song X. and Yunjun L., Effect of hyperbranched polyesters on htpb polyurethane curing kinetic, Materials Research, 2014, 17, 78-82.
[32] Elwell M.J., Ryan A.J., Grünbauer H.J. and Van Lieshout H.C., An ftir study of reaction kinetics and structure development in model flexible polyurethane foam systems, Polymer, 1996, 37, 1353-1361.